LARGE EDDY SIMULATION OF THE OCEAN MIXED LAYER: THE EFFECTS OF WAVE BREAKING AND LANGMUIR CIRCULATION

Yign Noh, Hong Sik Min
Department of Atmospheric Sciences,
Yonsei University
Shinchon-dong, Seodaemun-gu, Seoul 120-749, Korea
noh@atmos.yonsei.ac.kr, hsmin@atmos.yonsei.ac.kr

Siegfried Raasch
Institute for Meteorology and Climatology
University of Hannover
Herrenhäuser Street 2, Hannover 30419, Germany
rash@muk.uni-hannover.de

ABSTRACT

Large eddy simulation (LES) of the ocean mixed layer was performed in which both wave breaking and Langmuir circulation are realized. High resolution simulations were carried out using parallel computing, with or without each contribution, wave breaking and Langmuir circulation, with an aim to clarify their respective roles in the ocean mixed layer. The effects of wave breaking were found to be mainly limited to the near surface zone of the upper few meters. Langmuir circulations below it are not significantly modified, although they become somewhat weakened and less coherent. Under the influence of wave breaking, however, the turbulence production in the upper ocean mixed layer becomes dominated by the TKE flux, contrary to the case of the atmospheric boundary layer, which is in good agreement with the result from the ocean mixed layer model.

INTRODUCTION

The most significant characteristic of the ocean mixed layer in contrast to the atmospheric boundary layer is the presence of wave breaking and Langmuir circulation at the free surface.

Recent measurements revealed that wave breaking causes the dissipation rate of turbulence near the sea surface to be ~2 orders larger than expected from the classical logarithmic boundary layer near the rigid surface, and the roughness length scale at the sea surface to be in the range of 0.1 - 8 m, much larger than that of the atmospheric boundary layer (see, Melville, 1998).

There is a large amount of documents that witnessed Langmuir circulations since Langmuir (1938) (see, Leibovich 1983). According to Craik and Leibovich (1976), the formation of Langmuir circulation is initiated by the interaction of the Stokes drift with the wind-driven surface shear current, which can be realized by an additional 'vortex force' term in the momentum equation as $\boldsymbol{u}_s \times \boldsymbol{\omega}$, where $\boldsymbol{u}_s$ is Stokes drift velocity and $\boldsymbol{\omega}$ is vorticity. Meanwhile, McWilliams et al. (1997) suggested a turbulent Langmuir number La_t as the relevant parameter for the occurrence of Langmuir circulation in the turbulent ocean mixed layer as

$$La_t = (u_* / U_s)^{1/2} \qquad (1)$$

where U_s is the Stokes drift velocity at the surface and u_* is the frictional velocity.

Considering the strong turbulence near the surface generated by wave-breaking and the large scale eddies associated with Langmuir circulations, it is natural to suspect that both wave breaking and Langmuir circulation may play important roles in the vertical mixing process in the ocean mixed layer. Nonetheless, their effects have not been taken into consideration in most ocean mixed layer models developed (see, for example, Large, 1998), although several attempts are made recently to incorporate these effects into the ocean mixed layer models (Noh and Kim, 1999; D'Alessio et al., 1998; Burchard, 2001 and Li and Garrett, 1997).

The development of an appropriate LES model for the ocean mixed layer has been hindered by the difficulty of handling the boundary condition at the sea surface, in which wave breaking and Langmuir circulations are present. Skyllingstad and Denbo (1995) and McWilliams et al. (1997) successfully reproduced Langmuir circulations in the ocean mixed layer by applying the Craik and Leibovich's theory (1976) recently, but no attempt has been made yet to include the effects of wave breaking in the LES of the ocean mixed layer.

In this paper we attempted to accomplish the LES of the ocean mixed layer in which both wave breaking and Langmuir circulation are realized, with an aim to clarify their respective roles in the ocean mixed layer. We also compared the dissipation rate and the TKE flux at the surface with observation data to confirm the validity of the LES results. Finally, we compared the LES results with the one dimensional ocean mixed layer model (OMLM) by Noh and Kim (1999).

LES MODEL AND SIMULATIONS

The LES model we used in this study is developed based on the PALM, whose parallel code shows an excellent performance up to very large number of processors (Raasch and Schröter, 2001). Subgrid-scale turbulence is modeled according to Deardorff (1980). A periodic boundary condition at the side, a free slip boundary condition at the surface, and a radiation condition at the bottom were applied, respectively.

The momentum equation is modified by following the theory by Craik and Leibovich (1976). Wave breaking is an extremely complicated phenomenon whose realistic simulation requires a resolution much higher than that of LES. Meanwhile, as long as

we are concerned with the dynamical process in the ocean mixed layer influenced by wave breaking rather than wave breaking itself, it may suffice if we can simulate the turbulence generated by wave breaking instead of simulating the wave breaking process directly. Therefore, in this paper we introduced the near surface turbulence generated by wave breaking in the LES model by imposing a small-scale random velocity fluctuation at the sea surface whose velocity and length scales are consistent with the observed ones in the real ocean

The modified momentum equation is then given by

$$\frac{\partial u_i}{\partial t} = -(u_j + u_{sj})\frac{\partial u_i}{\partial x_j} - \frac{1}{\rho_0}\frac{\partial p}{\partial x_i} - \varepsilon_{ijk} f_j (u_k + u_{sk}) + \varepsilon_{ijk} u_{sj} \omega_k + \nu \frac{\partial^2 u_i}{\partial x_j \partial x_j} + F_i(\mathbf{x}, t) \quad (2)$$

Here the random forcing F_i is given by a Gaussian random forcing $G(x,y,t)$ whose integral length and time scales are given by l_0 and, τ_0 corresponding to those of the near surface small-scale turbulence generated by wave breaking; i.e.,

$$F_i = \frac{\alpha u_*}{\tau_0} G(x,y,t)\delta(z)(1-\delta_{i3}) \quad (3)$$

where α is a proportional constant. In this case, the rate of energy input by random forcing can be estimated as (Alvelius 1999),

$$\int_0^{\Delta z}\int_{-\infty}^{\infty} \overline{F_i(t)F_i(t')}\, dt'\, dz \cong \frac{(\alpha u_*)^2}{2\sqrt{\pi}\tau_0}\Delta z \quad (4)$$

when F_i is uncorrelated to u_i. Here Δz is the thickness of the first grid.

The value of α = 3.0 was determined so as to be consistent with the observed dissipation profile near the sea surface. We also assumed the length scale of turbulence at the surface as l_0= 1.25 m in our model. The time scale forcing τ_0 was determined by $\tau_0 = 0.1\ l_0 / \alpha u_*$.

Assuming a homogeneous, steady, monochromatic wave field, the associated Stokes velocity was given by

$$u_s = U_s \exp(-4\pi z / \lambda) \quad (5)$$

with $U_s = (\pi a/\lambda)^2 (g\lambda/2\pi)^{1/2}$, where a is the wave height, λ is the wave length, and g is the gravitational acceleration. For wave height and wavelength, we used typical values such as a = 1.0 m and λ = 40 m.

The model domain was 300 m in the horizontal direction (x and y) and 80 m in the vertical direction (z). The number of grid point was 240 x 240 x 64, and the corresponding grid sizes were 1.25 m in both horizontal and vertical directions. The wind stress was given by a constant friction velocity u_* = 0.01 ms^{-1}, which results in La_t= 0.45. The Coriolis force was given by f= 10^{-4} s^{-1}, and the density was assumed to be constant.

To investigate the effects of wave breaking and Langmuir circulation in the ocean mixed layer, we carried out four different experiments; cases with both effects (EXP XA), with none of these effects (EXP O), with only wave breaking (EXP X), and with only Langmuir circulation (EXP A).

RESULTS

The Velocity Field And Its Vertical Profiles

Fig. 1 presents the instantaneous vertical velocity fields from EXP O and EXP XA at horizontal cross-sections with increasing depths (z = 1.25 m, 10 m, 25, and 50 m).

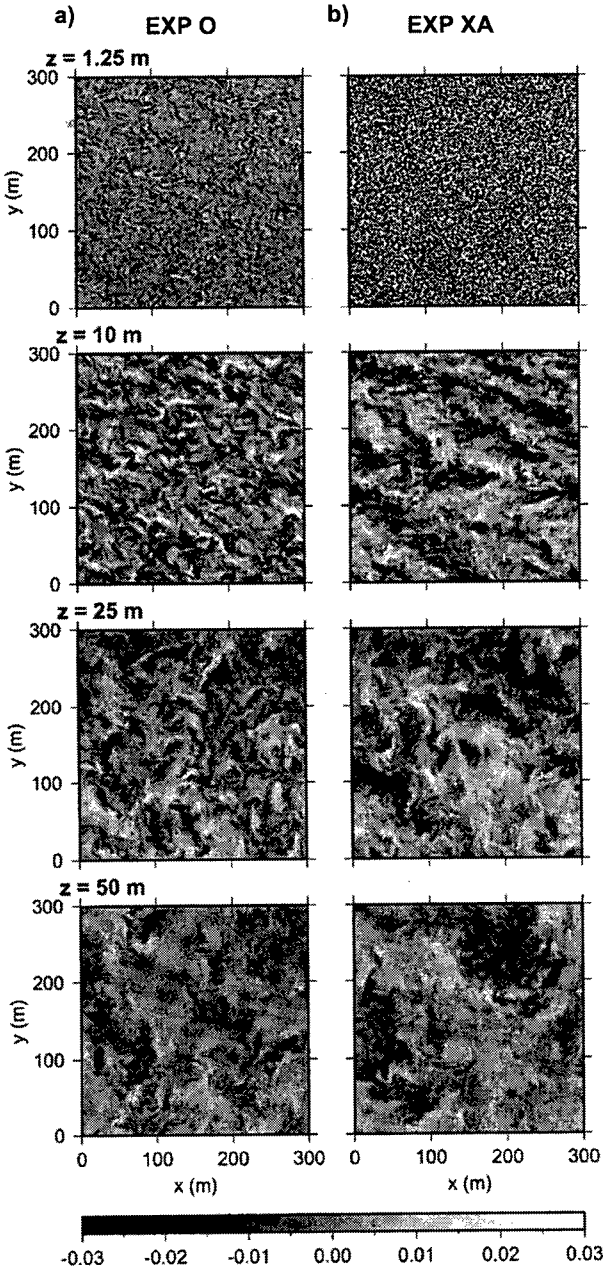

Fig. 1. Distributions of vertical velocity at the horizontal cross-sections (z = 1.25, 10, 25, 50 m); (a) EXP O, (b) EXP XA.

In EXP XA, streaks of the strong downwelling zone beneath the surface convergence appear up to $z \sim \lambda$, associated with Langmuir circulation. The direction of stripes spirals clockwise toward a diagonal orientation with increasing depths, and the distance between the stripes increases with depths. Meanwhile, the velocity fields near the surface are dominated by much stronger small-scale turbulence generated by wave breaking, although the Langmuir circulation pattern below the near surface zone remains relatively unaffected by the presence of wave breaking in agreement with observation (Gemmrich and Farmer 1999).

The results from EXP A show similar features as those from EXP XA, except the presence of strong small-scale turbulence near the surface. Nevertheless, Langmuir cells tend to become weaker and less coherent in the presence of wave breaking.

On the other hand, in the absence of a vortex force (EXP O), no organized structure appears, although the velocity field is weakly aligned along the wind direction near the surface. However, with increasing depths, the velocity field becomes more isotropic and the length scale increases. The results from EXP X are not significantly different to those from EXP O, except the presence of strong small-scale turbulence near the surface.

The distinctive features of the ocean mixed layer can be also clearly identified in the instantaneous vertical velocity fields in vertical cross-sections (Fig. 2), where strong downward plumes associated with Langmuir circulation are clearly observed in EXP XA.

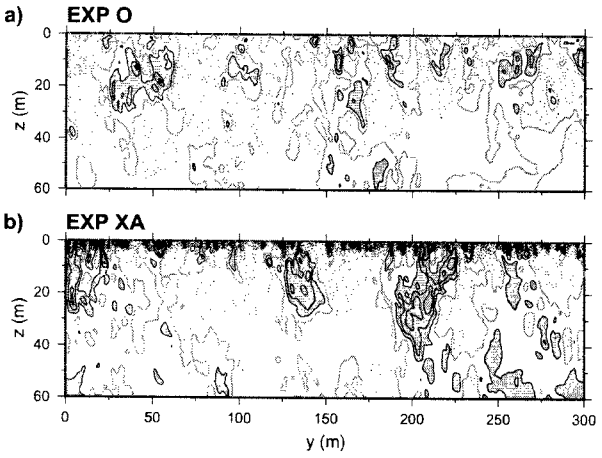

Fig. 2. Distributions of vertical velocity at the vertical cross-sections.). Contour levels are 0.01 ms^{-1}. Solid lines represent the downward velocity, and dotted lines represent the upward one. Here the regions in which the downward velocity exceeds 0.01 ms^{-1} are shaded; (a) EXP O, (b) EXP XA.

Mean Vertical Profiles of TKE and Velocity

The effects of wave breaking and Langmuir circulation can be clearly evidenced in the vertical profiles of the mean TKE (Fig. 3) and of the mean horizontal velocities (Fig. 4). In particular, TKE below the near surface zone is substantially increased in the presence of Langmuir circulation, but it is smaller in EXP XA than EXP A (Fig. 3). It was also found that very effective vertical mixing of momentum occurs down to much deeper depths in the presence of Langmuir circulation (Fig. 4).

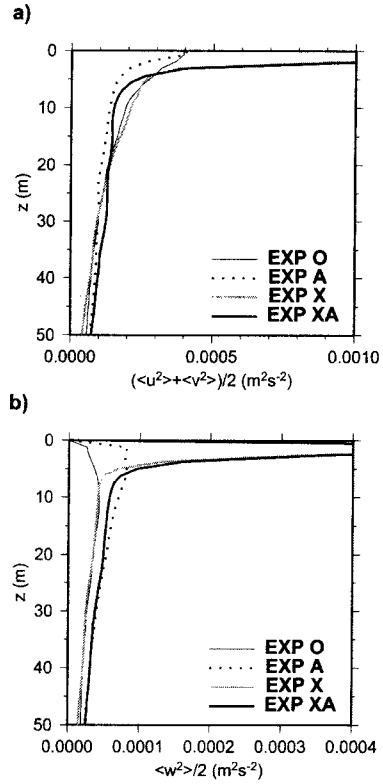

Fig. 3. Profiles of the mean horizontal TKE (a) and the mean vertical TKE (b) from each experiment.

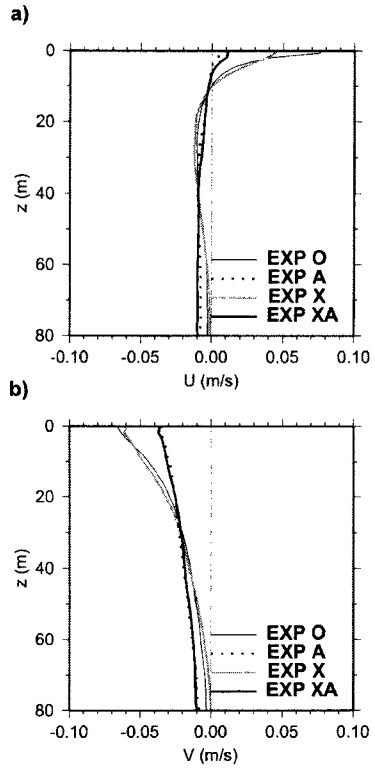

Fig. 4. Profiles of the mean horizontal velocity; (a) U, (b) V.

Spectrum of The Vertical Velocity Field

Fig. 5 compares horizontal spectra of the vertical velocity field Φ_w at various depths in the ocean mixed layer (z = 1.25, 2.5, 7.5, 12.5, 25, 50 m) (EXP O, EXP XA). Expectedly, the small-scale turbulence dominates near the surface in the presence of wave breaking. In the deeper layer (z = 7.5, 12.5, 25, 50 m), the levels of the spectrums at low wave numbers in EXP A and EXP XA are substantially higher than those of EXP O and EXP X, as a result of Langmuir circulation.

The inertial subrange of the spectrum, which follows the Kolmogorov spectrum $k\Phi_w \propto \varepsilon^{2/3}k^{-2/3}$, appears in the spectra at depths larger than z = 7.5 m for all experiments, thus confirming the premise of LES. On the other hand, in the near surface zone, where small-scale turbulence generated by wave breaking dominates, the inertial subrange does not appear within the grid resolution of the present simulation.

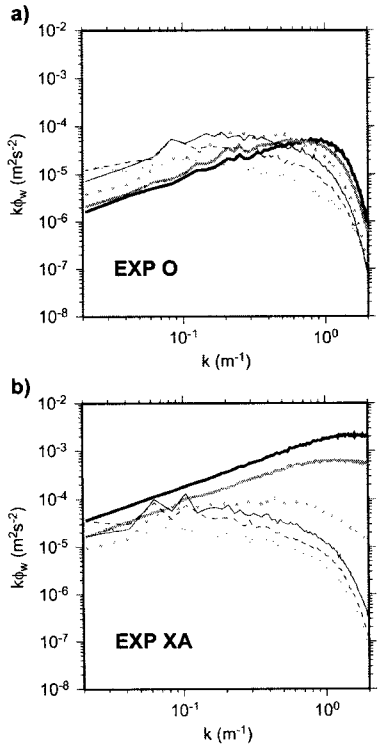

Fig. 5. Horizontal wave number spectra of the vertical velocity Φ_w at various depths in the ocean mixed layer (▬ : z = 1.25 m, ▬ : 2.5 m, ▬ : 7.5 m, ▬ : 12.5 m, ▬ : 25 m, ▬ : 50 m); (a) EXP O, (b) EXP XA.

Mean Profiles of Dissipation Rate

Based on the observation data, Craig and Banner (1996) suggested that the dissipation rate near the surface is estimated as

$$\varepsilon = \frac{2.4Au_*^3}{z_0}\left(1+\frac{z}{z_0}\right)^{-3.4} \qquad (6)$$

while it restores the scaling of the logarithmic boundary layer ($\varepsilon = u_*/\kappa z$, with the von Karman constant κ) away from the surface. Here A is a proportional constant.

Fig. 6 compares the profiles of dissipation rates with the estimation (6). For the case of α=0, we found that the LES data underestimate the dissipation rate by more than an order of magnitude, as in Skyllingstad et al. (1999). The dissipation rate increases in the near surface with increasing α. The close agreement with the observation data is found when α = 3.0.

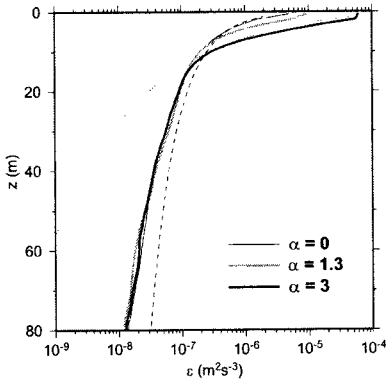

Fig. 6. Profiles of the dissipation rates; ▬ : the scaling for the wall layer, ▬ : the scaling by Craig and Banner (1994) (6), ▬ : LES (α= 0), ▬ : LES (α = 0.8), ▬ : LES (α = 4.0).

Comparison With An Ocean Mixed Layer Model (OMLM)

Noh and Kim (1999) suggested an OMLM, which is based on the turbulence closure based on the eddy viscosity, similarly to Mellor and Yamada (1982), but takes into account the effects of wave breaking by applying much larger values for the TKE flux (F = mu_*^3) and the length scale at the sea surface (z_0) (see also Noh et al., 2002). Noh and Kim (1999) suggested the values as m = 100 and z_0 = 1 m, in consistence with Craig and Banner (1994). Here we adjusted the value of m as $m \cong 80$ from the estimation (3) with α = 3.0. It has been suggested by Craig and Banner (1994) based on the analysis of the observation data that the enhancement of the TKE flux at the surface owing to wave breaking renders the downward TKE flux dominant in the TKE budget of the upper mixed layer, contrary to the case of the atmospheric boundary layer where shear production dominates. The profiles of TKE budget, obtained from the OMLM with wave breaking (m = 80, z_0 = 1 m) and without it (m = 0, z_0 = 0 m), clearly evidence the contrasting features mentioned above (Fig. 7).

Taking the above results into account, we examined the TKE budgets obtained from EXP O and EXP XA, as shown in Fig. 8. The results clearly show the dominance of the shear production and the TKE flux in the TKE budget of the upper mixed layer, respectively, in good agreement with the OMLM results shown in Fig. 8. It was also found that Langmuir circulation suppresses shear production too, although the dominance of the TKE flux is mainly due to wave breaking.

CONCLUSION

In this paper, we performed for the first time a LES of the ocean mixed layer, in which both wave breaking and Langmuir circulation are realized, and clarified their respective roles in the ocean mixed layer.

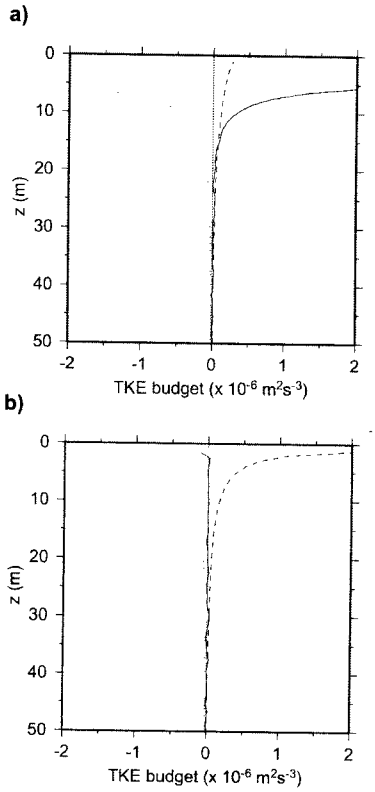

Fig. 7. Profiles of the terms of TKE budget from the OMLM (——: TKE flux, – – ·: shear production, ····· : dissipation rate); (a) $m = 80$, $z_0 = 1$ m, (b) $m = 0$, $z_0 = 0$ m.

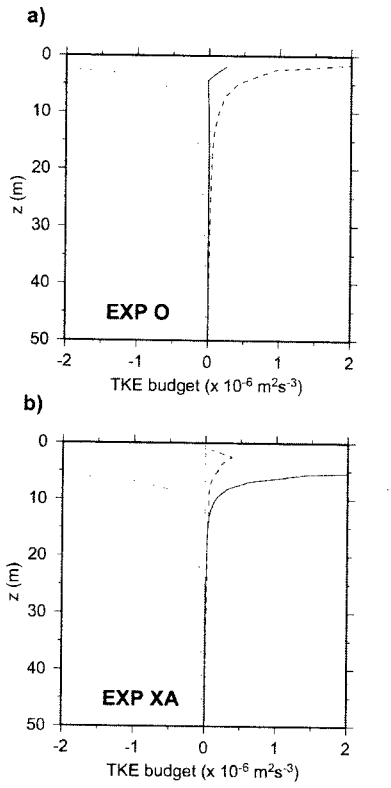

Fig. 8. Profiles of the terms of TKE budget from the LES (—— : TKE flux, – – ·: shear production, ····· : dissipation rate); (a) EXP O, (b) EXP XA.

REFERENCES

Alvelius, K., 1999, "Random forcing of three-dimensional homogeneous turbulence", *Phys. Fluids*, 11, 1880-1889.

Burchard, H., 2001, "Simulating the wave-enhanced layer under breaking waves with two-equation turbulence models", *J. Phys. Oceanogr.*, 31, 3133-3145.

Craig, P. D., and M. L. Banner, 1994, "Modeling wave-enhanced turbulence in the ocean surface layer", *J. Phys. Oceanogr.*, 24, 2546-2559.

Craik, A. D. D., and S. Leibovich, 1976, "A rational model for Langmuir circulations", *J. Fluid Mech.*, 73, 401-426.

Deardorff, J. W., 1980, "Stratocumulus-capped mixed layers derived from a three-dimensional model", *Boundary-Layer Meteorol.*, 18, 495-572.

Gemmrich, J. R., and D. M. Farmer, 1999. "Near-surface turbulence and thermal structure in a wind-driven sea", *J. Phys. Oceanogr.*, 29, 480-499.

Large, W. G., 1998, "Modeling and parameterizing ocean planetary boundary layers", *Ocean Modeling and Parameterization* (ed. E.P. Chassignet and J. Verron, Kluwer Acad. Pub.), pp. 81-120.

Leibovich, S., 1983, "The form and dynamics of Langmuir circulation", *Annu. Rev. Fluid. Mech.*, 15, 391-427.

Li, M., and C. Garrett, 1997, "Mixed layer deepening due to Langmuir circulation", *J. Phys. Oceanogr.*, 27, 121-132.

McWilliams, J. C., P. P. Sullivan, and C. H. Moeng, 1997, "Langmuir turbulence in the ocean", *J. Fluid Mech.*, 334, 1-30.

Mellor, G. L., and T. Yamada, 1982, "Development of a turbulent closure model for geophysical fluid problems", *Rev. Geophys. Space Phys.*, 20, 851-875.

Melville, W. K., 1996, "The role of surface-wave breaking in air-sea interaction", *Annu. Rev. Fluid. Mech.*, 28, 279-321.

Noh, Y., and H. J. Kim, 1999, "Simulations of temperature and turbulence structure of the oceanic boundary layer with the improved near-surface process", *J. Geophys. Res.*, 104, 15621-15634.

Noh, Y., C. J. Jang, T. Yamagata, P. C. Chu, and C. H. Kim, 2002, "Simulation of more realistic upper ocean process from OGCM with a new ocean mixed layer model", *J. Phys. Oceanogr.*, 32, 1284-1507.

Raasch, S., and M. Schröter, 2001, "A large eddy simulation model performing on massively parallel computers", *Z. Meteorol.* 10, 363-372.

Skyllingstad, E. D., and D. W. Denbo, 1995, "An ocean large-eddy simulation of Langmuir circulations and convection in the surface mixed layer", *J. Geophys. Res.*, 100, 8501-8522.

Skyllingstad, E. D., W. D. Smyth, J. N. Moum, and H. Wijesekera, 1999, "Upper-ocean turbulence during a westerly wind burst: A comparison of large-eddy simulation results and microstructure measurements", *J. Phys. Oceanogr.*, 29, 5-28.